Hindawi
International Journal of Polymer Science
Volume 2019, Article ID 5738613, 10 pages
https://doi.org/10.1155/2019/5738613

Research Article

High-Efficiency DNA Extraction Using Poly(4,4′-Cyclohexylidene Bisphenol Oxalate)-Modified Microcrystalline Cellulose-Magnetite Composite

Aisha Nawaf Al balawi,[1,2] **Nor Azah Yusof**,[1,3] **Sazlinda Kamaruzaman**,[1] **Faruq Mohammad**,[4] **Helmi Wasoh**,[5] **and Hamad A. Al-Lohedan**[4]

[1]*Department of Chemistry, Faculty of Science, Universiti Putra Malaysia, 43400 UPM Serdang, Selangor, Malaysia*
[2]*Haql College, University of Tabuk, 71491 Tabuk, Saudi Arabia*
[3]*Institute of Advanced Technology, Universiti Putra Malaysia, 43400 UPM Serdang, Selangor, Malaysia*
[4]*Surfactants Research Chair, Department of Chemistry, College of Science, King Saud University, 11451 Riyadh, Saudi Arabia*
[5]*Faculty of Biotechnology and Biomolecular Science, Universiti Putra Malaysia, 43400 UPM Serdang, Selangor, Malaysia*

Correspondence should be addressed to Nor Azah Yusof; azahy@upm.edu.my and Faruq Mohammad; fmohammad@ksu.edu.sa

Received 22 November 2018; Revised 17 January 2019; Accepted 29 January 2019; Published 4 June 2019

Academic Editor: Hossein Roghani-Mamaqani

In this study, we studied the DNA extraction capability of poly(4,4′-cyclohexylidene bisphenol oxalate) following the surface modification and composite formation with that of microcrystalline cellulose (MCC) and magnetic iron oxide nanoparticles (NPs). The physical characterization techniques like scanning electron microscopy (SEM), Fourier-transform infrared (FTIR) spectroscopy, energy-dispersive X-ray analysis (EDX), and thermogravimetric analysis (TGA) were employed for the poly(bisphenol Z oxalate)-MCC-magnetite composite during different stages of its formation. The results confirmed the successful modification of the polymer surface. On testing in the presence of three types of binding buffers, a high value of 72.4% (out of 10,000 ng/μL) efficiency with a total yield of DNA at 2×10^6 ng and absorbance ratio of A260/A280 (1.980) was observed for the 2 M GuHCl/EtOH binding buffer. These results were compared against the other two buffers of phosphate-buffered saline (PBS) and NaCl. The lowest value of DNA extraction efficiency at 8125 ng/μL of 58.845% with absorbance ratios of A260/A280 (1.818) for PBS was also observed. The study has concluded an enhancement in the DNA extraction efficiency when the polymer is in the composite stage along with cellulose and magnetite particles as compared against the bare polymer.

1. Introduction

In recent years, nanocomposites have been extended to many different fields because of their greater potentials and ability to enhance the fundamental characteristics of any basic material. The nanocomposites in general are formed as a combination of two or more materials of different origins. For example, the polymer nanocomposites contain polymeric organics with metal/inorganic nanoparticles (NPs), while the magnetic nanocomposites are ferromagnetic or superparamagnetic materials such as iron, cobalt, and nickel with a diameter of 50-200 nm [1]. Several types of polymer nanocomposites have got interest in many studies such as polyester/nanoclay [2], silicates [3], graphene [4], carbon nanotubes (CNTs) [5], and magnetic polymer beads [6]. One important sector among many different applications of nanocomposites that employ polymeric matrices includes the DNA isolation and purification process.

The process to extract DNA is the first and essential step to do some activities that hold importance in the molecular biology such as hybridization, sequencing, ligation, amplification, biodetection, and cloning. The applications of the

DNA isolation technique are several and a few of them include the gene therapy, forensic science applications, diagnosis of diseases, and pathogen detection [7–9]. The chemistry and other related properties of DNA molecule structures help to separate and purify it through several methods [7, 10, 11]. The purification methods include the conventional methods that involve the use of fluid-phase to be phenol/chloroform mixture and cetyltrimethylammonium bromide (CTAB) and developmental methods such as solid-phase (e.g., glass fibers, silica, magnetic particles, and CNTs) [9]. Previous studies have discussed the methods to enhance the isolation efficiency of DNA by solid supports; for instance, Shakhmaeva et al. [10] studied the DNA adsorption by using CNTs as solid-phase extraction (SPE) sorbents. Other studies included the isolation of plant DNA using phenol-stacked CNTs [11], poly(hydroxyethyl methacrylate)-magnetite particles to DNA purification from *Escheria coli* [12], magnetic nanoparticles (MNPs) with *N*-isopropylacrylamide (NIPAM) for DNA adsorption [13], and DNA isolation using hemoglobin-modified magnetic nanocomposite as solid-phase adsorbents [14].

Solid-phase support of nanocomposites involves the extraction and purification of DNA and has several advantages over the conventional methods like high accuracy, sensitivity, increased surface area for immobilization of DNA, and reduced time of incubation [15]. In addition, the isolation techniques involving the MNPs display benefit in limited use of chemicals, sustainable costs, minor physical or chemical damage, and ease of automation. The adsorption of DNA on polymer nanocomposite (solid-supported) takes place through driving force of hydrophobic, hydrogen bonding, and electrostatic interaction. These bondings are associated with functional groups (–COOH, –OH, and $–NH_2$) of MNPs that have been surface-modified including coated with inorganic materials (e.g., iron oxide, silica, and gold) for investigation of high-efficiency loading (isolation) [16]. Polymer nanocomposites have been distinguished from other solid support materials because of the polymers with NPs new class and possess advanced properties with multiple applications. The overall characteristics and performances are determined based on the concentration and type of functional groups (e.g., carboxylic, iminodiacetate, amine, and sulfonic), structure of polymer, and methods to prepare polymer nanocomposites [17]. Moreover, the other surface influential physical properties of the polymer nanocomposites like surface area, micropore size, shape, and porosity play a crucial role towards the adsorption and isolation of DNA [18].

The present study has provided a novel process of producing the polymer nanocomposites that include magnetically responsive metal oxide and microcrystalline cellulose (MCC) for the extraction of high-efficiency DNA. Following the composite formation, the physicochemical techniques to fully understand the structure of poly(4,4′-cyclohexylidene bisphenol oxalate) having a benzene ring and oxygen bond to form covalent bonding with the iron oxide MNPs were studied by different instrumental techniques. Finally, the subsequent adsorption of DNA by the surface-modified polymer in the presence of three different buffers has also been studied.

2. Experiment

2.1. Materials. The DNA solution used as DNA specimen in this study was purchased from Sigma Company (D7290). Iron oxide (Fe_3O_4) with the particle size 50-100 nm, MCC with 20 μm particle size, urea, HNO_3, and all other solvents were purchased from (Sigma-Aldrich). All the reagents used in this study were of the highest analytical grade (≥95%), which were received and utilized with no further purification. For the synthesis of poly(4,4′-cyclohexylidene bisphenol oxalate), we adopted the condensation-polymerization method where the product was obtained in form of white powder [19].

2.2. Synthesis of Poly(4,4′-Cyclohexylidene Bisphenol Oxalate)-MCC-Fe_3O_4 Composite. About 4.5 g of poly(4,4′-cyclohexylidene bisphenol oxalate) was added to 90 mL ultrapure water followed by the sonication for 15 min and cooled to 0°C by placing the reaction mixture in a refrigerator. In the next step, 6 g NaOH, 4 g urea, and 4 g MCC were added to the frozen suspension and stirred, and 4.5 g of Fe_3O_4 powder was added with stirring. The reaction mixture was kept in an ice bath for 10 min and then cooled to -20°C for 2 hours. After the period, the mixture was taken out from the cooler and 1 mL of 2 M HNO_3 was added at room temperature and stirred for 30 min. After this, 1 mL of 2 M HNO_3 was added to the composite and was left inside the acid overnight. This step was followed by washing the solution with distilled water for 15 min. Later, the synthesized composite was filtered and dried.

2.3. DNA Extraction Using the Polymer Nanocomposite. The study has used 2 M of guanidine hydrochloride (GuHCl) in 96% ethanol (EtOH), 2 M NaCl solution, and phosphate-buffered silane (PBS, 5 M GuHCl in 30% propanol) as three binding buffers for measuring the binding capacity of poly(4,4′-cyclohexylidene bisphenol oxalate)-MCC-Fe_3O_4 composite for the DNA analysis. A 200 μL of DNA solution (20 μL DNA and 180 μL of deionized water) was mixed with 300 μL binding buffer, whereas two different weights (0.2 g and 0.4 g) of poly(4,4′-cyclohexylidene bisphenol oxalate)-MCC-Fe_3O_4 composite were inserted into an Eppendorf tube including binding buffer and DNA solution with a total volume of 500 μL, followed by the incubation for 10 min. The solution was taken out using a pipette and washed with 70% EtOH to clean all the salts from the surface. The elution was separated from the modification of polymer, while the efficiency and purity of the assessing the DNA extraction was carried out in the elusion buffer.

3. Purity and Yield Analysis of Extracted DNA

For the high-purity DNA, we measured the absorbance ratio between 260 nm and 280 nm using a nanophotometer device ranging from 1.8 to 2.0. In order to calculate the

total purity and extraction efficiency of DNA, we used the following equations:

$$\begin{aligned} &\text{Total yield of DNA purification} \\ &\quad = \text{Final elution of the solution's volume} \\ &\qquad \times \text{DNA concentration } (\mu L), \end{aligned} \tag{1}$$

$$\begin{aligned} &\text{Extraction efficiency} \\ &\quad = \text{Total DNA yield/total DNA amount} \\ &\qquad \cdot (\text{ng/input DNA volume}, \mu L). \end{aligned} \tag{2}$$

4. Characterization of the Modified Polymer

For the Fourier-transform infrared (FTIR) spectroscopy analysis where it indicates the functional groups and bonding of the polymer at different stages of its formation, the PerkinElmer Spectrum 100 FTIR instrument was employed. For the analysis, the samples were recorded in the range of 4000-400 cm^{-1} using KBr pellets. The Mettler Toledo instrument was applied to investigate the thermal stability of the polymer nanocomposite in the range of 60-700°C by means of thermogravimetric analysis (TGA) and differential thermogravimetry (DTG). The scanning electron microscopy (SEM) technique was used to observe the changes in the surface morphology of the polymer composite using a Module NOVA NANOSEM 230 – FE 1™ instrument. The electron diffraction analysis by X-rays (EDAX) instrument with a Module NOVA NANOSEM 230 – FE 1™ was used for the elemental analysis. Lake Shore 7400 series was employed with vibrating sample magnetometer (VSM) to measure the magnetic properties of poly(4,4′-cyclohexylidene bisphenol oxalate)-MCC-Fe_3O_4 composite. The UV-Vis spectroscopic analysis was measured by the NanoDrop 2000 spectrophotometer.

5. Results and Discussion

Mixed polymer, NaOH, urea, MCC, and Fe_3O_4 powder cooled at -20°C condition were then dropped by HNO_3 that resulted in the formation of a black powder having the magnetic properties. Such formed polymer composite along with the starting materials was analyzed by FTIR spectroscopy, and the results are shown in Figure 1. The surface-modified composite, poly(4,4′-cyclohexylidene bisphenol oxalate)-MCC-Fe_3O_4, resulted in the observation of bands for stretching vibration of the carbonyl group (C=O) in the polymer around 1725 cm^{-1} and the broad peak around 3270 cm^{-1} can be assigned to the C-H stretching vibrations of the cyclohexane of polymer. The C=C stretching vibrations from all the samples (except Fe_3O_4) were observed in the range of 1600-1658 cm^{-1}, meaning that the functional groups related to C=C from the monomer, polymer, and cellulose are maintained in the polymer composite too. Also, the C-O-C group appeared in the finger print region of around 1012-1045 cm^{-1} is an indicative of the presence of carboxy-related groups from both polymer and cellulose in the final composite. The broadband in the composite around 1378 cm^{-1} is due

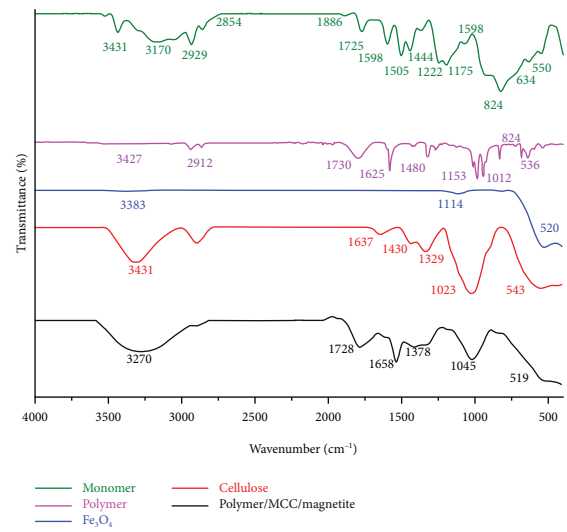

Figure 1: FTIR spectral comparison of poly(4,4′-cyclohexylidene bisphenol oxalate)-MCC-Fe_3O_4 composite, with that of pure polymer and pure iron oxide.

to the bending vibrations of C-H groups, and the same band was observed as a sharp peak in the cellulose material around 1329 cm^{-1} due to the availability of a less number of C-H groups as compared to the final composite. Similarly, the observation of peak around 520 cm^{-1} in the samples of Fe_3O_4 and the polymer composite can be assigned to the Fe-O stretching bands of magnetite material [20]. From the comparison and analysis of all other spectral bands, it can be confirmed that the poly(4,4′-cyclohexylidene bisphenol oxalate)-MCC-Fe_3O_4 sample maintains the functional groups of polymer, Fe_3O_4, and MCC, which further confirms for the successful formation of the polymer composite.

The TGA and DTG curves for the final polymer composite were compared with those of the pure polymer and pure iron oxide, and the results have been shown in Figures 2(a) and 2(b). From Figure 2(a), it can be observed that the polymer after its composite formation due to the inclusion of Fe_3O_4 seems to have slight variations in the multistep thermal degradation pattern. For the polymer composite, the first decomposition temperature of polymer was observed between 58°C and 94°C, with sample loss of 4%, and 52.41 to 1567°C, with sample loss of 7% for the surface-modified polymer. The second thermal decomposition event started between 103°C and 223°C with sample loss of 12.5%, while surface modification of polymer observed sample loss of 14% between 157°C and 338°C. The last step to decomposition of polymer and surface modification of polymer was limited at 226-624°C with the sample remained to be 81%, and in the temperature range of 351-672°C, the sample amount remained to be around 71%. Similarly, the analysis of TGA results for the other samples indicated to have a weight loss of more than 95% and only 14% for the pure polymer and pure Fe_3O_4, respectively. These results are anticipated when dealing with the pure organic and metal containing samples where there is no solid-supported content in the polymer and

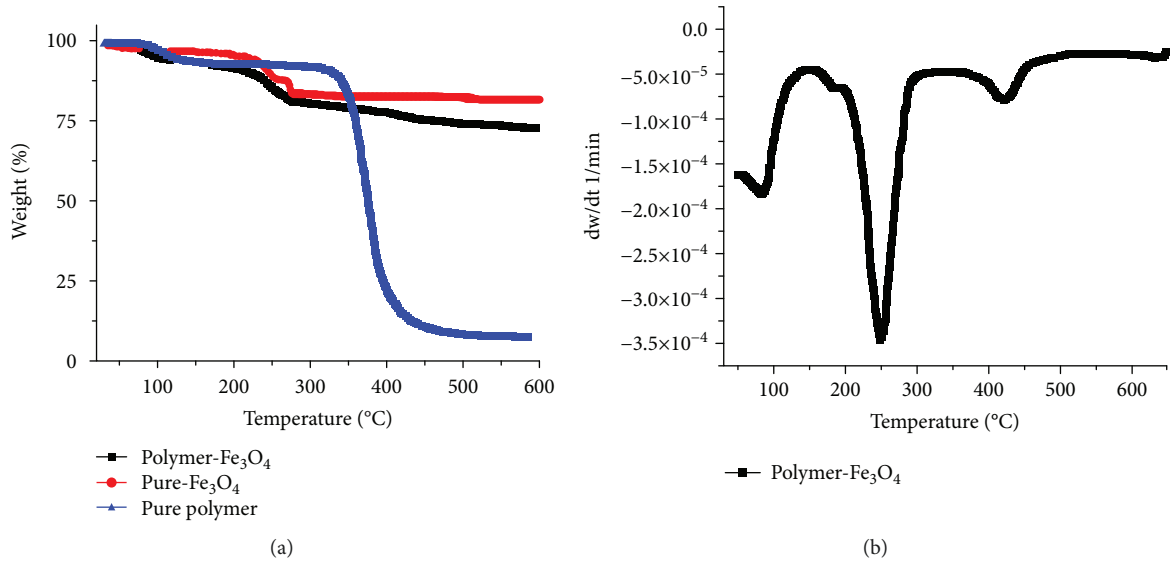

Figure 2: (a) TGA and (b) DTG analysis of the final polymer composite with that of pure polymer and pure iron oxide.

Table 1: TGA and DTG of surface modification of the polymer.

Pyrolysis temperature	Weight loss
86.53°C	0.26 mg
249.63°C	1.98 mg
424.96°C	0.29 mg

organic content in the iron oxide material. In that way, the observation of the remained amount of 71% for the polymer composite sample is confirmed to have the remaining 29% as the polymer content, i.e., each 100 mg of polymer composite has about 71 mg of Fe_3O_4 and 29 mg of organic content. Further, the DTG curve (Figure 2(b)) for the polymer composite observed the integral peak around 86°C and loss of 0.26 mg as the beginning of the pyrolysis of polymer nanocomposite. The second integral peak was at 249°C with a mass loss of 1.98 mg, and the last pyrolysis reaction polymer nanocomposite was at 425°C, where the mass loss is 0.29 mg (Table 1).

5.1. Morphological Characterization. Figures 3(a)–3(c) have illustrated the surface modification of the polymer composite characterized by SEM and EDAX analysis. It is observed that the polymer before composite formation (Figure 3(a)) has a large gap and rough surface, which turned to be smoother and smaller beads shaped following its composite formation (Figure 3(b)). The formation of the composite in the beads shape following the surface modification can be attributed to the presence of MCC, while the magnetite presence was supporting the particle's agglomeration. The average particle size of the beads was observed to be 136 nm, and the standard deviation for this particles was 45.74, while the average particle size of polymer before modification was 162 nm and they were uniform with slight agglomeration. The appearance of peaks for the respective elements in the sample confirmed the presence of Fe, O, and C from the EDAX analysis (Figure 3(c)). This provided enough evidence for the successful formation of the composite proposed in the present study.

The surface area of poly(4,4′-cyclohexylidene bisphenol oxalate)-MCC-Fe_3O_4 composite was measured by BET analysis, and the results have been shown in Figure 4 and Table 2. In this procedure, the N_2 gas was used for the physical adsorpion, and for the analysis, the bath was maintained at 77.251 K. From Figures 4(a) and 4(b), the formation of IUPAC was classified through the appearance of isotherm linear plot type III adsorption model. Table 2 has shown three very important values to study the surface area of polymer composite like pore volume, total surface area, and pore size. It was observed that the N_2-mediated BET surface area of the polymer composite was 2.6549 m^2/g. However, the surface area for the polymer before modification was measured to be 1.9294 m^2/g, which indicated increase in the surface area value. The results showed that the single-point adsorption and desorption total pore volume were 0.181943 cm^3/g and 0.198761 cm^3/g, respectively (Table 2). The pore sizes (adsorption and desorption average pore diameter) by (4 V/A by BET) were 2741.2863 Å and 2994.6726 Å, but for polymer before modification, it was 2426.3042 Å (242.63 nm) indicating an increase in the pore size (Table 2). Therefore, majority of the pores were classified into the range of macroporous with an average pore diameter of 242.63 nm. This helped in classifying IUPAC on pore dimensions, whereas three kinds of the pore dimensions of adsorbents were grouped as the micropore ($d < 2$ nm), the mesopore (d = 2-50 nm), and the macropore ($d > 50$ nm).

5.2. Magnetic Properties of Poly(4,4′-Cyclohexylidene Bisphenol Oxalate)-MCC-Fe_3O_4 Composite. Figures 5(a) and 5(b) have illustrated the magnetic hysteresis curves of pure Fe_3O_4 with those of poly(4,4′-cyclohexylidene bisphenol oxalate)-MCC-Fe_3O_4 composite measured by static hysteresis graph. From the comparison of both graphs, it is observed that the superparamagnetic property of the magnetite material (Figure 5(a)) is getting persisted in the polymer composite too (Figure 5(b)) as indicated by the generation of magnetic

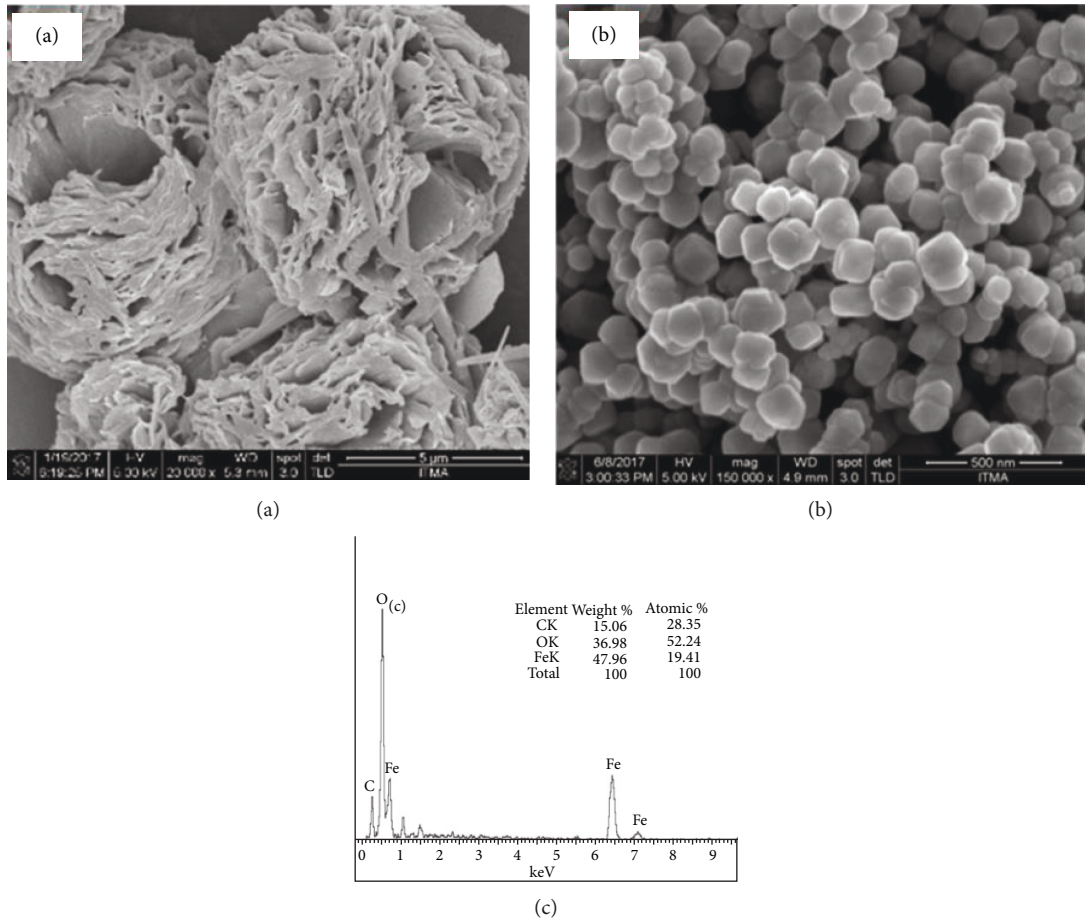

Figure 3: SEM images of poly(4,4′-cyclohexylidene bisphenol oxalate) (a) and poly(4,4′-cyclohexylidene bisphenol oxalate)-MCC-Fe_3O_4 composite (b). The EDAX analysis of the final composite is shown in (c).

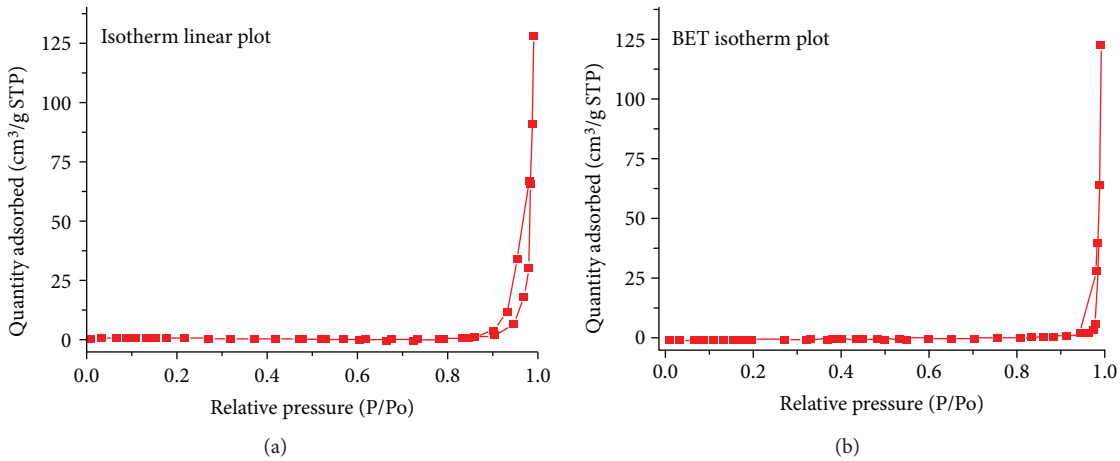

Figure 4: (a) BET isotherm linear plot for polymer composite. (b) Isotherm linear plot for polymer composite.

hysteresis loops. The highest magnetization value observed for the pure magnetite material has to be 83.55 emu/g while for the polymer composite to be 36.7 emu/g only. Such a decrease in the total saturation magnetization values for the polymer composite as compared against the pure magnetite material can be attributed to the presence of polymer in the composite. In general, the presence of polymer material onto the surface of magnetic core material usually decreases the total oscillation of the particles due to an increase in the polymer weight present at the surface

Table 2: The values of surface area and pore volume for poly(4,4′-cyclohexylidene bisphenol oxalate).

Relative pressure (P/P_0)	Surface area	BET surface area	Single-point adsorption total pore volume of pores less than 842.856 Å radius	Single-point desorption total pore volume of pores less than 928.410 Å radius	Pore size (adsorption and desorption average pore diameter) by (4 V/A by BET)
0.271	1.4475 m^2/g	2.6549 m^2/g	—	—	—
0.988	—	—	0.181943 cm^3/g	—	
0.989	—	—	—	0.198761 cm^3/g	2,741.2863 Å and 2,994.6726 Å

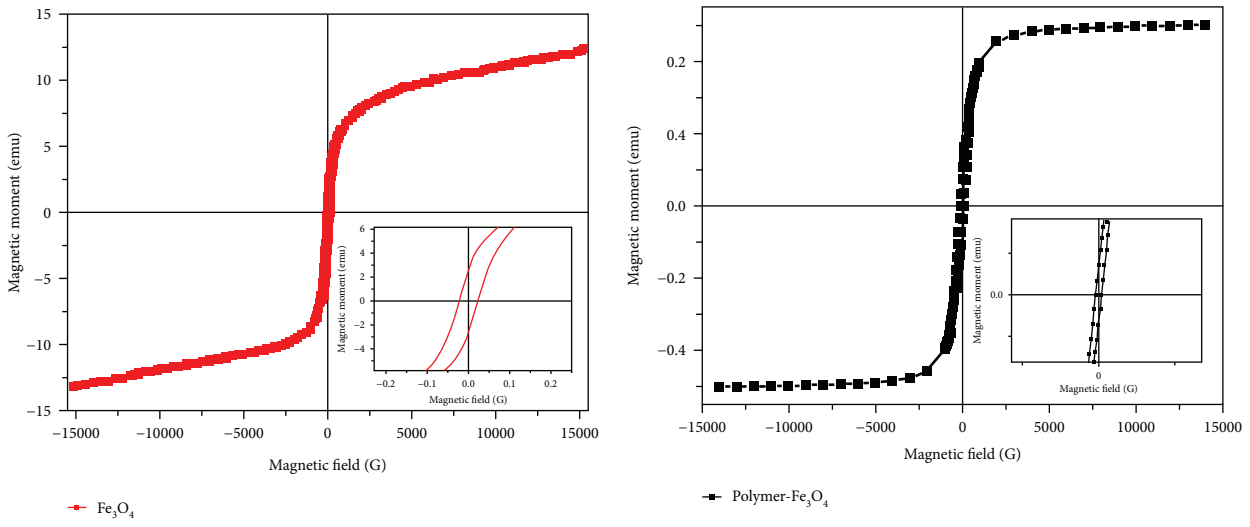

Figure 5: Comparison of the magnetic hysteresis loops of (a) pure iron oxide and (b) poly(4,4′-cyclohexylidene bisphenol oxalate)-MCC-Fe_3O_4 composite.

Table 3: The values of saturation magnetization (M_s) and coercivity (H_c) for the poly(4,4′-cyclohexylidene bisphenol oxalate)-MCC-magnetite composite.

Sample	Saturation magnetization (M_s) (emu/g)	Coercivity (H_c) (G)	Retentivity (M_r) (emu/g)
Poly(4,4′-cyclohexylidene bisphenol oxalate)-MCC-magnetite composite	36.70	99.88	5.36

of the magnetic material [20, 21]. The observation of such property can be used to extrapolate the composite's application to various other different fields like magnetic hyperthermia-based therapy and drug delivery. The various other magnetic properties like saturation magnetization (M_s), coercivity (H_c), and retentivity (M_r) for the poly(4,4′-cyclohexylidene bisphenol oxalate)-MCC-Fe_3O_4 composite are presented in Table 3.

According to the obtained results, the value of H_c and the value of M_s were comparable with the values of M_s and H_c as depicted in the previous study [22]. The M_s of the Kenaf/magnetite40/polyester composite was 29.2 emu/g that was smaller than the M_s value obtained in the present study. However, the H_c was 112.2 Oe – (112.2 G) was higher than the results (99.88 G) proposed in the present study. Doulabi et al. [23] stated that M_s and H_c for $Ni_{0.3}Zn_{0.7}Fe_2O_4$ polyvinyl acetate nanocomposite were 4.31 emu/g and 368.39 G, respectively, while the polymer composite in the present study was 36.70 emu/g and 99.88 G.

Typek et al. [24] measured the M_s and H_c values for the nanopowder sample, and the results of their study indicated that the M_s value was smaller than the present study results; however, the H_c values were higher. As compared to other studies, the observation of such decreased H_c values for composite in the present study can be attributed to the formation of composite structure with high

Table 4: Comparison of the extraction efficiencies of pure polymer, poly(4,4′-cyclohexylidene bisphenol oxalate) with that of poly(4,4′-cyclohexylidene bisphenol oxalate)-MCC-magnetite composite.

Binding buffer	Sample weight	Pure polymer extraction efficiency (ng/μL)	Polymer composite extraction efficiency (ng/μL)
2 M GuHCl/EtOH	0.2 g	2247.5	7237.5
PBS	0.2 g	875	7177.5
2 M NaCl	0.2 g	1692.52	7222.5

molecular weights onto the surface of the magnetite particles that probably affect the magnetic properties [21, 25].

5.3. Extraction Efficiency and Purity of DNA. The comparison of the DNA extraction efficiency among the polymer before and after modification has been presented in Table 4, where the results confirmed improvement in the efficiency for all the tested conditions. The observation of such results can be attributed to an increase in the surface area due to the beads formed as part of the composite formation as against the pure polymer without the bead structure.

Table 5 has described the values of DNA extraction efficiency for the polymer composite, when tested under different weights and buffered conditions. It has been noted that there was no major difference in the percentage efficacy for all the three buffers tested and the values follows the order of GuHCl > NaCl > PBS of binding buffers at 0.4 g in the samples. Moreover, significant improvement was observed in the extraction efficiency with that of the polymer weighted. The values of absorbance ratios indicated high purity of DNA with higher extraction efficiency. A comparison of the maximum extraction efficiency and total yield of the modification of polymer NPs with those of some other affinity matrices has been provided in Table 6. The modification of polymer NPs showed high extraction efficiency for ssDNA (single-stranded DNA) at 10,000 (ng/μL) with total yield 2×10^6 ng. This indicated that the modification of polymer NPs had a sufficient affinity to capture the ssDNA. The differences of ssDNA purification and total yield amounts were dependent on the properties of adsorbent such as functional groups, structure, pore size of particles, surface area, and ligand density.

The objective of this study was to examine the effect of magnetic iron oxide-coated polymer composite towards the extraction of DNA, and for that, we have prepared the superparamagnetic Fe_3O_4-coated with MCC and poly(4,4′-cyclohexylidene bisphenol oxalate). The physical characterization of the prepared composite provided the information that the Fe_3O_4 particles are firmly surrounded by the MCC and poly(4,4′-cyclohexylidene bisphenol oxalate) polymer. This provides a primary evidence that there will not be any toxic effect for the direct interaction of the Fe_3O_4 particles with that of the bounded DNA, where the MCC and polymer serve as the protective shield from the oxidative behavior of iron, since the DNA possesses some protein groups having electron-rich surfaces and its direct interaction with the electron-deficient iron (Fe^{2+} or Fe^{3+}) has a tendency to absorb the electrons from those protein groups, and in that way, there is a chance for the destabilization of the adsorbed DNA [33]. In our case, the surface-coated groups like MCC and the polymer inhibit such oxidative action of Fe_3O_4 while simultaneously maintain the superparamagnetic behavior of magnetite iron oxide particles (Figure 5). Further, we observed a significant enhancement in the adsorption of DNA for the magnetic polymer composite as compared against the pure polymer (Table 4) and this increased extraction efficiency for the composite can be attributed to the density and associated stability offered by the solid support [34], since the polymer particles bound to the solid iron oxide surfaces allow for their increased and continuous interaction with that of the DNA molecules and thus contributed for the enhanced efficiency. As shown schematically in Figure 6, the polymer coating available at the surface of Fe_3O_4 particles can hold the DNA molecules by means of multiple forces like physical adsorption and chemical bonding. For example, the magnetic force means of interaction of DNA's phosphate backbone structure with that of polymer sheets supported by the Fe_3O_4 particles increase the adsorption by π-π stacking which occurs between polymer and the nucleobase ring structures [35]. Also, the MCC makes as a bridge between DNA and polymer that play a key role to increase the number of hydrogen bonding which also supports for the enhanced efficiency. In the present case, we have selected the magnetite particles having two different oxidation states of Fe^{2+} and $Fe^{3+}$and tested the efficiency linked to the magnetic properties. The iron oxide NPs can be available in other isomeric forms too having different oxidation states and changes of magnetic properties, and so our future studies have to deal with the DNA extraction studies of other iron oxide bound polymer composites like wüstite, maghemite, and hematite.

6. Conclusion

The present study has analyzed the structure of poly(4,4′-cyclohexylidene bisphenol oxalate) having a benzene ring and oxygen bond forming covalent bonding with the magnetic iron oxide NPs. It has used Fe_3O_4 NPs for the modification of poly(4,4′-cyclohexylidene bisphenol oxalate) polymer by means of MCC and magnetite particles. The physicochemical properties of the formed composite were thoroughly studied by means of SEM, thermal analysis, FTIR, EDAX, and magnetic hysterisis. The DNA extraction for the polymer poly(4,4′-cyclohexylidene bisphenol oxalate)-MCC-magnetite nanocomposite indicated high efficiency, i.e., 10,000 ng/μL for 2 M GuHCl/ethanol of binding buffer. The absorbance ratios of A260/A280 at 0.4 g of polymer composite weight were 1.980, 1.818, and 2.100 for 2 M GuHCl/EtOH, PBS, NaCl, respectively, indicating a highly purified DNA following the extraction process. The study results have confirmed that the composite prepared in the present study is superior to many different materials applied for the DNA extraction study. The composite exhibits superparamagnetic property due to its magnetic content, which can be explored in the future studies for other applications like

Table 5: Extraction efficiencies and total yields of DNA for the polymer composite under different weights and binding buffers.

Binding buffer	Polymer weight	Concentration	260/280	Total yield (ng)	Extraction efficiency (ng/μL)	Extraction efficiency (%)
2 M GuHCl/EtOH	0.2 g	2895	1.810	1,447,500	7237.5	52.417%
PBS	0.2 g	2871	1.763	1,435,500	7177.5	51.983%
2871	0.2 g	2889	2.254	1,444,500	7222.5	52.309%
2 M GuHCl/EtOH	0.4 g	4000	1.980	2,000,000	10,000	72.424%
PBS	0.4 g	3250	1.818	1,625,000	8125	58.845%
2 M NaCl	0.4 g	3592	2.100	1,796,000	8980	65.037%

Table 6: Comparison of the adsorption capacities for ssDNA from literature.

Type of material	Adsorption capacity for ssDNA	Reference
Polystyrene beads	67 mg/g	[26]
Poly(glycidyl methacrylate) beads	90 μg/g	[27]
Fe_3O_4 NPs with polyethylene imine	69.2 mg/g	[28]
Polyethylene glycol dimethacrylate-glycidyl methacrylate	65.1 μg/g	[29]
Polyethersulfone membranes	10 mg/mL	[30]
Poly(hydroxyethyl methacrylate)-Fe_3O_4 MNPs	154 mg/g	[12]
Immobilized on MNPs as a SPE adsorbent	27.86 mg/g	[18]
N-Isopropylacrylamide-MNPs	83.40 mg/g	[13]
Diethylaminoethyl-Magarose as binding	8200 ng	[31]
Polyglycidyl methacrylate-ethylene glycol dimethacrylate beads	1.36 mg/mL	[32]

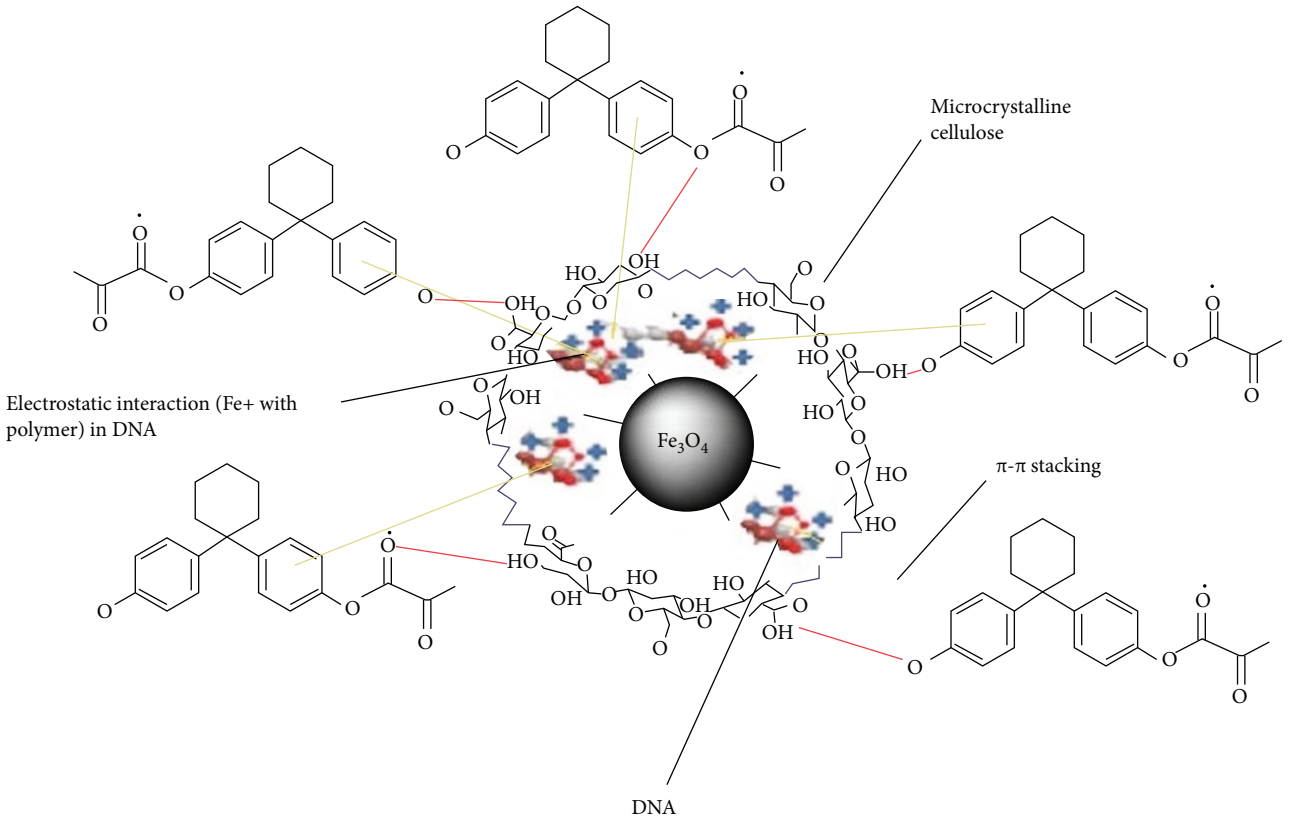

Figure 6: Schematic representation of the mechanism of adsorption and desorption of DNA onto the poly(4,4′-cyclohexylidene bisphenol oxalate)-MCC-Fe_3O_4 composite.

gene separation, magnetic hyperthermia-based therapy, and magnetically controlled drug delivery.

Data Availability

The datasets used and analyzed during the current study are available from the corresponding author on reasonable request.

Conflicts of Interest

The authors declare no conflict of interest.

Acknowledgments

The UPM authors are thankful to the Deputy Dean (DAR) of Universiti Putra Malaysia for the support. One of the authors, A.N.A.B., is grateful to the University of Tabuk for the financial support. The King Saud University authors are grateful to the Deanship of Scientific Research, King Saud University for funding through Vice Deanship of Scientific Research Chairs.

References

[1] M. Tadic, S. Kralj, M. Jagodic, D. Hanzel, and D. Makovec, "Magnetic properties of novel superparamagnetic iron oxide nanoclusters and their peculiarity under annealing treatment," *Applied Surface Science*, vol. 322, pp. 255–264, 2014.

[2] R. B. Valapa, S. Loganathan, G. Pugazhenthi, S. Thomas, and T. O. Varghese, "Chapter 2- an overview of polymer–clay nanocomposites," *Clay-Polymer Nanocomposites*, vol. 1, pp. 29–81, 2017.

[3] S. Gupta, P. C. Ramamurthy, and G. Madras, "Future scope of silicone polymer based functionalized nanocomposites for device packaging: a mini review," *Journal of Chemical Engineering & Process Technology*, vol. 6, no. 1, p. 213, 2015.

[4] A. Hussein and B. Kim, "Graphene/polymer nanocomposites: the active role of the matrix in stiffening mechanics," *Composite Structures*, vol. 202, pp. 170–181, 2018.

[5] J. Chen, B. Liu, X. Gao, and D. Xu, "A review of the interfacial characteristics of polymer nanocomposites containing carbon nanotubes," *RSC Advances*, vol. 8, no. 49, pp. 28048–28085, 2018.

[6] M. A. Ramazanov, F. V. Hajiyeva, A. M. Maharramov et al., "New magnetic polymer nanocomposites on the basis of isotactic polypropylene and magnetite nanoparticles for adsorption of ultrahigh frequency electromagnetic waves," *Polymer-Plastics Technology and Engineering*, vol. 57, no. 5, pp. 449–458, 2018.

[7] Y. Haddad, K. Xhaxhiu, P. Kopel, D. Hynek, O. Zitka, and V. Adam, "The isolation of DNA by polycharged magnetic particles: an analysis of the interaction by zeta potential and particle size," *International Journal of Molecular Sciences*, vol. 17, no. 4, p. 550, 2016.

[8] A. Abdulrahman and A. Ghanem, "Recent advances in chromatographic purification of plasmid DNA for gene therapy and DNA vaccines: a review," *Analytica Chimica Acta*, vol. 1025, pp. 41–57, 2018.

[9] R. Tao, S. Wang, J. Zhang et al., "Separation/extraction, detection, and interpretation of DNA mixtures in forensic science (review)," *International Journal of Legal Medicine*, vol. 132, no. 5, pp. 1247–1261, 2018.

[10] I. I. Shakhmaeva, E. R. Bulatov, O. V. Bondar et al., "Binding and purification of plasmid DNA using multi-layered carbon nanotubes," *Journal of Biotechnology*, vol. 152, no. 3, pp. 102–107, 2011.

[11] F. Nazarian-Firouzabadi, A. Ismaili, and S. M. Zabeti, "Phenol-stacked carbon nanotubes: a new approach to genomic DNA isolation from plants," *Molecular Biology Research Communications*, vol. 3, no. 3, pp. 205–213, 2014.

[12] I. Perçin, V. Karakoç, S. Akgöl, E. Aksöz, and A. Denizli, "Poly (hydroxyethyl methacrylate) based magnetic nanoparticles for plasmid DNA purification from *Escherichia coli* lysate," *Materials Science and Engineering: C*, vol. 32, no. 5, pp. 1133–1140, 2012.

[13] M. M. Rahman and A. Elaissari, "Temperature and magnetic dual responsive microparticles for DNA separation," *Separation and Purification Technology*, vol. 81, no. 3, pp. 286–294, 2011.

[14] X. W. Chen, Q. X. Mao, J. W. Liu, and J. H. Wang, "Isolation/-separation of plasmid DNA using hemoglobin modified magnetic nanocomposites as solid-phase adsorbent," *Talanta*, vol. 100, pp. 107–112, 2012.

[15] A. A. Topçu, S. Aşır, and D. Türkmen, "DNA purification by solid phase extraction (SPE) methods," *Hacettepe Journal of Biology and Chemistry*, vol. 3, no. 44, pp. 259–266, 2016.

[16] K. Kang, J. Choi, J. H. Nam et al., "Preparation and characterization of chemically functionalized silica-coated magnetic nanoparticles as a DNA separator," *The Journal of Physical Chemistry B*, vol. 113, no. 2, pp. 536–543, 2009.

[17] K. Akamatsu, S. Adachi, T. Tsuruoka, S. Ikeda, S. Tomita, and H. Nawafune, "Nanocomposite polymeric microspheres containing Ni nanoparticles with controlled microstructures," *Chemistry of Materials*, vol. 20, no. 9, pp. 3042–3047, 2008.

[18] B. A. Rozenberg and R. Tenne, "Polymer-assisted fabrication of nanoparticles and nanocomposites," *Progress in Polymer Science*, vol. 33, no. 1, pp. 40–112, 2008.

[19] S. T. Al-Hamidi, B. A. Sweileh, and F. I. Khalili, "Preparation and characterization of poly (bisphenol A oxalate) and studying its chelating behavior towards some metal ions," *Solvent Extraction and Ion Exchange*, vol. 26, no. 2, pp. 145–162, 2008.

[20] F. Mohammad and N. A. Yusof, "Doxorubicin-loaded magnetic gold nanoshells for a combination therapy of hyperthermia and drug delivery," *Journal of Colloid and Interface Science*, vol. 434, pp. 89–97, 2014.

[21] C. S. S. R. Kumar and F. Mohammad, "Magnetic gold nanoshells: stepwise changing of magnetism through stepwise biofunctionalization," *The Journal of Physical Chemistry Letters*, vol. 1, no. 20, pp. 3141–3146, 2010.

[22] C. Xia, K. Wang, Y. Dong et al., "Dual-functional natural-fiber reinforced composites by incorporating magnetite," *Composites Part B: Engineering*, vol. 93, pp. 221–228, 2016.

[23] F. S. Doulabi, M. Mohsennia, and S. Taraghikhah, "Synthesis and characterization of magnetic $Ni_{0.3}$ $Zn_{0.7}$ Fe_2O_4/polyvinyl acetate (PVAC) nanocomposite," *Journal of Polymer Engineering*, vol. 34, pp. 823–828, 2014.

[24] J. Typek, K. Wardal, G. Zolnierkiewicz et al., "Magnetic studies of 0.7 (Fe_2O_3)/0.3(ZnO) nanocomposites in nanopowder form and dispersed in polymer matrix," *Materials Science-Poland*, vol. 34, no. 2, pp. 286–296, 2016.

[25] S. A. Gomez-Lopera, R. C. Plaza, and A. V. Delgado, "Synthesis and characterization of spherical magnetite/biodegradable polymer composite particles," *Journal of Colloid and Interface Science*, vol. 240, no. 1, pp. 40–47, 2001.

[26] C. Paril, D. Horner, R. Ganja, and A. Jungbauer, "Adsorption of pDNA on microparticulate charged surface," *Journal of Biotechnology*, vol. 141, no. 1-2, pp. 47–57, 2009.

[27] H. P. Zhang, S. Bai, L. Xu, and Y. Sun, "Fabrication of monosized magnetic anion exchange beads for plasmid DNA purification," *Journal of Chromatography B*, vol. 877, no. 3, pp. 127–133, 2009.

[28] C. L. Chiang, C. S. Sung, T. F. Wu, C. Y. Chen, and C. Y. Hsu, "Application of superparamagnetic nanoparticles in purification of plasmid DNA from bacterial cells," *Journal of Chromatography B*, vol. 822, no. 1-2, pp. 54–60, 2005.

[29] Y. Han and G. M. Forde, "Single step purification of plasmid DNA using peptide ligand affinity chromatography," *Journal of Chromatography B*, vol. 874, no. 1-2, pp. 21–26, 2008.

[30] M. A. Teeters, S. E. Conrardy, B. L. Thomas, T. W. Root, and E. N. Lightfoot, "Adsorptive membrane chromatography for purification of plasmid DNA," *Journal of Chromatography A*, vol. 989, no. 1, pp. 165–173, 2003.

[31] P. R. Levison, S. E. Badger, J. Dennis et al., "Recent developments of magnetic beads for use in nucleic acid purification," *Journal of Chromatography A*, vol. 816, no. 1, pp. 107–111, 1998.

[32] L. Wu and G. C. Pang, "High-speed large scale chromatographic purification of plasmid DNA with a novel giant-pore stationary phase," *Chromatographia*, vol. 66, no. 3-4, pp. 151–157, 2007.

[33] F. Mohammad and N. A. Yusof, "Surface ligand influenced free radical protection of superparamagnetic iron oxide nanoparticles (SPIONs) toward H9c2 cardiac cells," *Journal of Materials Science*, vol. 49, no. 18, pp. 6290–6301, 2014.

[34] F. Mohammad, T. Arfin, and H. A. Al-Lohedan, "Enhanced biological activity and biosorption performance of trimethyl chitosan-loaded cerium oxide particles," *Journal of Industrial and Engineering Chemistry*, vol. 45, pp. 33–43, 2017.

[35] A. P. Tiwari, S. J. Ghosh, and S. H. Pawar, "Biomedical applications based on magnetic nanoparticles: DNA interactions," *Analytical Methods*, vol. 7, no. 24, pp. 10109–10120, 2015.